Phase Synchronization for Helix Enhanced Wake Mixing in Downstream Wind Turbines

van Vondelen, Aemilius A.W.; Ottenheym, Joris; Pamososuryo, Atindriyo K.; Navalkar, Sachin T.; van Wingerden, Jan Willem

DOI
10.1016/j.ifacol.2023.10.1039

Publication date
2023

Document Version
Final published version

Published in
IFAC-PapersOnLine

Available online at www.sciencedirect.com

ScienceDirect

IFAC Papers Online CONFERENCE PAPER ARCHIVE

IFAC PapersOnLine 56-2 (2023) 8426–8431

Phase Synchronization for Helix Enhanced Wake Mixing in Downstream Wind Turbines

Aemilius A.W. van Vondelen * **Joris Ottenheym** *
Atindriyo K. Pamososuryo * **Sachin T. Navalkar** **
Jan-Willem van Wingerden *

* *Delft University of Technology, Delft, 2628 CD Delft, The Netherlands (e-mail: {A.A.W.vanVondelen, J.Ottenheym, A.K.Pamososuryo, J.W.vanWingerden}@tudelft.nl)*

** *Siemens Gamesa Renewable Energy, Prinses Beatrixlaan 800, 2595 BN The Hague, The Netherlands (email: Sachin.Navalkar@siemensgamesa.com)*

Abstract: Wind farm controllers such as the Helix approach have shown potential in increasing plant power production through wake mixing. The concept suggests that actuating the upstream turbines' blade pitching with a specific periodic signal can induce a helix-shaped wake, thereby alleviating wind velocity deficit on downstream turbines. Wake mixing initiation by downstream turbines may also be shown advantageous for power production; however, little to no attention has been given to such an approach. Similar wake mixing is expected to be achievable at lower control costs if the downstream turbine can benefit from the periodic component already present in the wake of the upstream turbine. Such a hypothesis is studied in this work by designing a minimal control scheme where the wake acting on the downstream turbine is simulated by a periodic input disturbance. A Kalman filter is proposed for incoming input disturbance phase estimation using SCADA data. The reconstructed phase information allows synchronization of the downstream control action with the periodic input disturbance by means of a phase synchronization wake mixing controller. The periodic component was estimated with a minimal root-mean-square error and the resulting control action was in phase with the input disturbance and demonstrated satisfactory performance even with a small phase perturbation. Future work will include applications in a high-fidelity wind turbine model and wind tunnel studies.

Keywords: Wake Mixing, Helix, Downstream Turbine, Kalman Filter, Phase Estimation

1. INTRODUCTION

One of today's main challenges is the transition towards clean energy (Pörtner et al., 2022). Wind energy has grown to be one of the main solution pathways in this challenge, due to its increasing cost-effectiveness (Global Wind Energy Council, 2022). The most important method through which cost reduction can be achieved is by increasing the capacity of a turbine by enlarging its rotor, often enabled by innovations in control (Van Kuik et al., 2016). Another method is by placing turbines together in arrays such that maintenance and infrastructure costs can be shared. Yet, a significant disadvantage of grouping turbines is the occurrence of a phenomenon called the wake effect, which takes place when downstream turbines are aligned with the wake of an upstream turbine causing a reduction in the overall energy production of the wind farm (see e.g. González-Longatt et al. (2012); Barthelmie et al. (2009)).

The wake is a low-velocity turbulent region directly behind the upstream turbine, which eventually mixes again with the ambient wind flow to recover energy. Wind farm layouts are usually optimised for this wake effect. Nonetheless, for some wind farms, the wake effect can still increase fatigue significantly and reduce the total potential power production by up to 20% (Barthelmie et al., 2009).

Wind farm control addresses the wake effect while considering farm-level objectives, thereby reducing overall loading and increasing total performance. This could imply reducing the performance or increasing the loading on a few turbines to benefit the entire farm. One preliminary idea to mitigate the wake effect is derating the upstream turbine, such that the downstream turbine experiences a higher wind velocity, a method known as Axial Induction Control (Annoni et al., 2016; van der Hoek et al., 2019). Another method, currently the only one commercially applied, purposely misaligns the upstream turbines from the wind direction to steer away the wake from the downstream turbines, hence it is referred to as wake steering or wake adapt (Fleming et al., 2014; Siemens Gamesa, 2019).

More recently proposed methods influence the wake dynamically to enhance wake mixing, such as Dynamic In-

10.1016/j.ifacol.2023.10.1039

duction Control (Goit and Meyers, 2015) and the Helix approach (Frederik et al., 2020). The Helix approach is a particularly promising method, as the actuation deviates only slightly from the normal operational envelope. Additionally, the performance decrease of the upstream turbine is small with moderately increased loading whilst the farm-level performance can be increased significantly (Frederik et al., 2020; Frederik and van Wingerden, 2022; van Vondelen et al., 2023). At the current state of research, wake-mixing methods have been studied predominantly for a two-turbine wind farm with an upstream turbine employing wake mixing and a downstream turbine employing baseline control, as illustrated in Fig. 1.

This study proposes periodic wake mixing control on the upstream *and* downstream turbines simultaneously thus benefiting turbines further downstream as well. Accordingly, some considerations come into play. First, as the upstream turbine employs the Helix approach, there is a periodic component in the wake. The downstream turbine experiences this periodic component on its structure, resulting in a periodic load. Second, when a turbine employs wake mixing control, similar periodic loads are created on its structure to actuate the flow. It is therefore expected that, for wake mixing on the downstream turbine, the loads caused by the periodic component in the incoming helix-shaped wake *and* the loads created by employing wake mixing should be synchronized. For example, without synchronization, the wake mixing that the downstream turbine is trying to achieve might be cancelled by the periodic component in the upstream turbine's wake when they are out of phase. As a result, it is expected that the downstream turbine can benefit from the gain of the periodic component in the wake, hence requiring less control action to achieve the same amount of wake mixing.

Phase synchronization can be achieved when knowledge of the wake's phase is available. However, the available knowledge in this work is limited to the excitation frequency of the upstream turbine's wake mixing controller, and SCADA data, representing a regular wind farm setup. Previous work on estimating wind field components include the use of a Kalman filter to estimate the effective wind speed (Simley and Pao, 2016). However, as the dynamics are modelled as a random walk, this approach is expected to be less suited to capture periodic wakes. Another work focused on a Kalman filter design for estimating periodic tower loading with slowly-varying amplitude and phase offset with respect to the driving excitation frequency (Pamososuryo et al., 2022). The estimation framework of the study relies on a model demodulation transformation, by which first-principle nonlinear wind turbine dynamics are recast as linear parameter-varying, scheduled by the excitation frequency. Several approaches also exist for phase synchronization of electricity grids, for example using a weighted least-squares estimator (Zheng et al., 2016). Although a potentially interesting approach for wind turbines since it is model-free, feedback stability issues might arise due to its output-only character if the control action is not in phase with the input. A Kalman filter appears a more suitable candidate for out-of-phase or any other control action since it can provide an unbiased and minimum variance estimate of the unknown input sequence. This work proposes a novel approach by modelling the periodic dynamics in an augmented state-space system, similar to how Greś et al. (2021) applied this to modal analysis, and subsequently synchronizing using the phase estimated by a Kalman filter.

Summarizing, the following contributions are presented in this work:

(1) We derive an augmented state-space system including the unknown periodic component of the incoming wake and propose a Kalman Filter for estimation of the augmented state.
(2) We present a phase synchronization wake mixing control scheme for the downstream turbine.
(3) We evaluate 1) and 2) on a simple three-degree-of-freedom system as proof of principle.

The remainder of this paper is organized as follows. Section 2 abstracts the downstream turbine to a mass-spring-damper system. Section 3 subsequently derives the augmented state-space model and proposes the Kalman filter estimator with a phase synchronization controller. Proceeding, the proposed controller is evaluated on a simple three-degree-of-freedom system as a proof of principle in Section 4 before conclusions are drawn in Section 5.

2. SYSTEM ABSTRACTION

This section derives the heavily simplified system representing a downstream turbine experiencing a helix-shaped wake. For this simplified representation, a mass-spring-damper system is chosen. The dynamics of a wind turbine pitch system are abstracted to an n degree-of-freedom linear time-invariant (LTI) mass-spring-damper system excited by r external forces representing the force generated by the wake. The equations of motion are then given by:

$$M\ddot{q}(t) + J\dot{q}(t) + Kq(t) = f(t), \tag{1}$$

where $f(t) \in \mathbb{R}^r$ is the external excitation force; $\ddot{q}(t), \dot{q}(t)$, and $q(t) \in \mathbb{R}^n$ are the acceleration, velocity, and displacement states, respectively; M, J, and $K \in \mathbb{R}^{n\times n}$ are the mass, damping and stiffness matrices, respectively. A linear model, as given above, covers only a small range of the nonlinear wind turbine system, and multiple of these models would be required to cover the full operating range. An alternative approach would be to use, e.g., linear parameter varying (LPV) or nonlinear models.

By taking the state and input vector as:

$$x(t) = \begin{bmatrix} q(t) \\ \dot{q}(t) \end{bmatrix} \in \mathbb{R}^{2n}, \quad u(t) = f(t), \tag{2}$$

the following state-space model is found:

$$\begin{aligned} \dot{x}(t) &= \underbrace{\begin{bmatrix} 0 & I \\ -M^{-1}K & -M^{-1}J \end{bmatrix}}_{A} x(t) + \underbrace{\begin{bmatrix} 0 \\ M^{-1} \end{bmatrix}}_{B} u(t) + w(t), \\ &= Ax(t) + Bu(t) + w(t), \end{aligned} \tag{3}$$

where $A \in \mathbb{R}^{2n\times 2n}$ is the state matrix, $B \in \mathbb{R}^{2n\times r}$ is the input matrix, and $w(t) \in \mathbb{R}^{2n}$ is the process noise. All states can be measured and collected in an output vector $y(t) \in \mathbb{R}^l$ with l outputs as follows:

$$y(t) = C^{\mathrm{a}}\ddot{q}(t) + C^{\mathrm{v}}\dot{q}(t) + C^{\mathrm{d}}q(t) + v(t), \tag{4}$$

where $C^{\mathrm{a}}, C^{\mathrm{v}}$, and C^{d} are the output location matrices for acceleration, velocity, and displacement, respectively,

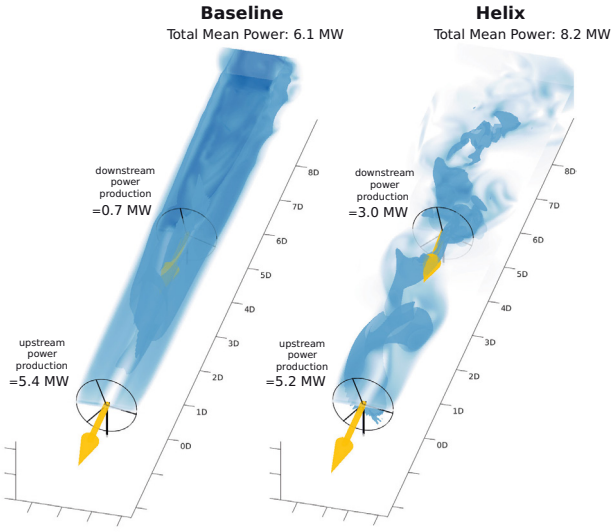

Fig. 1. Illustration of the Helix approach (right) during full wake overlap in a two turbine setup compared to a baseline case (left), data from an LES study from (Frederik et al., 2020), image cropped from (Meyers et al., 2022). The velocity magnitude is illustrated in light blue, whereas the isosurface of velocity is illustrated in dark blue. The x-axis represents the turbine spacing normalized for rotor diameter D.

and $v(t) \in \mathbb{R}^l$ is the measurement noise. For simplicity, the system will only be observed at the accelerations. This yields the following observation equation:

$$\begin{aligned} y(t) &= \underbrace{\begin{bmatrix} -C^{\mathrm{a}}M^{-1}K & -C^{\mathrm{a}}M^{-1}J \end{bmatrix}}_{C} x(t) + \underbrace{C^{\mathrm{a}}M^{-1}}_{D} u(t) + v(t), \\ &= Cx(t) + Du(t) + v(t), \end{aligned} \tag{5}$$

where $C \in \mathbb{R}^{l \times 2n}$ is the observation matrix and $D \in \mathbb{R}^{l \times r}$ is the feed-through matrix.

3. ESTIMATOR WITH PHASE SYNCHRONIZATION CONTROLLER

The periodic disturbance estimator with a phase synchronization controller is derived in this section. First, the periodic component of the incoming wake is modelled as a disturbance on the control input of the LTI mass-spring-damper system, derived in Section 2. Due to its stationarity, the periodic input disturbance can be included as deterministic system dynamics and therefore lacks load disturbance. Yet, certain stability conditions for a Kalman filter hold and it can therefore be applied, as suggested by Ni and Zhang (2013) and derived for an augmented LTI state-space system in Greś et al. (2021). By this inclusion, the disturbance can now be estimated as part of the augmented state using the Kalman filter. Now, the estimate's phase can be calculated and used to synchronize the control command with the incoming wake. The proposed control scheme is illustrated in Fig. 2.

3.1 Deriving the augmented state-space model

Here, the augmented model for Kalman filter state estimation of the system described by (3) and (5) is derived. First, the input can be partitioned as follows:

$$u(t) = \begin{bmatrix} u^{\mathrm{c}}(t) \\ u^{\mathrm{u}}(t) \end{bmatrix} + \begin{bmatrix} w^{\mathrm{c}}(t) \\ 0 \end{bmatrix}, \tag{6}$$

where $u^{\mathrm{c}}(t) \in \mathbb{R}^{r_c}$ and $u^{\mathrm{u}}(t) \in \mathbb{R}^{r_u}$, with $r = r_c + r_u$, correspond to the controllable and uncontrollable elements of u, respectively. The signal $w^{\mathrm{c}}(t) \in \mathbb{R}^{r_c}$ is the load disturbance acting on $u^{\mathrm{c}}(t)$. Unlike $u^{\mathrm{c}}(t)$, the uncontrollable input $u^{\mathrm{u}}(t)$ is generally unmeasured.

Correspondingly, the input and feedthrough matrices defined in Section 2 can thus be decomposed into:

$$B = \begin{bmatrix} B^{\mathrm{c}} & B^{\mathrm{u}} \end{bmatrix}, \quad D = \begin{bmatrix} D^{\mathrm{c}} & D^{\mathrm{u}} \end{bmatrix}, \tag{7}$$

where $B^{\mathrm{c}} \in \mathbb{R}^{2n \times r_c}$, $B^{\mathrm{u}} \in \mathbb{R}^{2n \times r_u}$, $D^{\mathrm{c}} \in \mathbb{R}^{l \times r_c}$, and $D^{\mathrm{u}} \in \mathbb{R}^{l \times r_u}$.

To model a periodic incoming wake, the assumption is made that the unmeasured and uncontrollable input of interest is purely periodic and the remaining input disturbance can be included in the load disturbance $w^{\mathrm{u}}(t) \in \mathbb{R}^{r_u}$:

$$u^{\mathrm{u}}(t) = \begin{bmatrix} u^{\mathrm{p}}(t) \\ 0 \end{bmatrix} + w^{\mathrm{u}}(t), \tag{8}$$

where $u^{\mathrm{p}}(t) \in \mathbb{R}^h$, with h the number of periodic components. In practice, the wake also contains harmonics of the excitation frequency, which can also be estimated if desired. Since the phase information of the fundamental excitation frequency is the main interest for the estimation problem, including this frequency only is sufficient. Moreover, as the goal is to amplify the unmeasured and uncontrollable periodic input through a control action, it is proposed to model this input as a disturbance *on the respective control input*. This way, the estimated signal simulates the control action that would cause a similar response as the disturbance is causing on the structure.

Next, it is assumed that the periodic component $u^{\mathrm{p}}(t)$ of the wind field can be modelled as:

$$u^{\mathrm{p}}(t) = \sum_{i=1}^{h} \alpha_i \sin(\omega_i t + \varphi_i), \tag{9}$$

where $\alpha_i, \varphi_i, \omega_i$ are the amplitude, phase shift, and frequency of the i-th periodic component. It is assumed that knowledge of the h frequencies is available. In practice, the excitation frequency of the upstream turbine is known, and the frequency of the wake does not appear to change over its trajectory (Frederik and van Wingerden, 2022).

The following step now is to treat these periodic components as dynamics in the state-space system such that augmentation with the original dynamics is possible. First, define a new set of states:

$$x^{\mathrm{p}}(t) = \begin{bmatrix} \alpha_1 \sin(\omega_1 t + \varphi_1) \\ \alpha_1 \cos(\omega_1 t + \varphi_1) \\ \vdots \\ \alpha_h \sin(\omega_h t + \varphi_h) \\ \alpha_h \cos(\omega_h t + \varphi_h) \end{bmatrix}, \tag{10}$$

such that,

$$u^{\mathrm{p}}(t) = \begin{bmatrix} 1 & 0 & \dots & 1 & 0 \end{bmatrix} x^{\mathrm{p}}(t). \tag{11}$$

where $x^{\mathrm{p}}(t) \in \mathbb{R}^{2h}$ is the periodic state. Subsequently, the first time-derivative of (10) is given by:

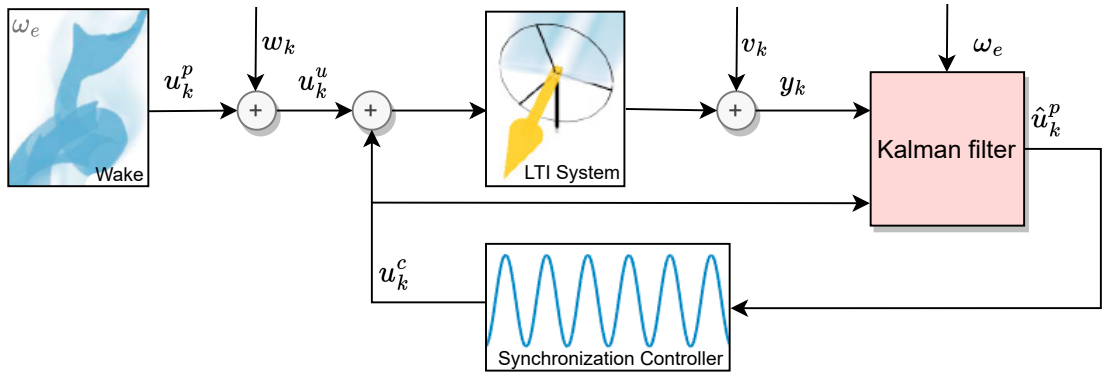

Fig. 2. Proposed control diagram. The wake is modelled as a periodic input disturbance u_k^{p} with known frequency ω_e and unknown phase acting on the control input channel u_k^{c}. A load disturbance w_k also acts on this channel. The output of the LTI system is disturbed by v_k and fed to the Kalman filter estimator together with the control input. The wake frequency ω_e is a known quantity used in the augmented system, which produces an estimate $\hat{u}_k^{\mathrm{p}}$ used for phase synchronization by the controller.

$$\dot{x}^{\mathrm{p}}(t) = \begin{bmatrix} \omega_1\alpha_1\cos(\omega_1 t+\varphi_1) \\ -\omega_1\alpha_1\sin(\omega_1 t+\varphi_1) \\ \vdots \\ \omega_h\alpha_h\cos(\omega_h t+\varphi_h) \\ -\omega_h\alpha_h\sin(\omega_h t+\varphi_h) \end{bmatrix}, \tag{12}$$

which can be written as the following dynamics:

$$\dot{x}^{\mathrm{p}}(t) = A^{\mathrm{p}}x^{\mathrm{p}}(t), \tag{13}$$

where A^{p} is given by:

$$A^{\mathrm{p}} = \mathrm{diag}(\Omega_1,\ldots,\Omega_h), \quad \text{where } \Omega_i = \begin{bmatrix} 0 & \omega_i \\ -\omega_i & 0 \end{bmatrix}. \tag{14}$$

Finally, (13) can be augmented with (3) and (5), resulting in the augmented state-space model:

$$\begin{bmatrix} \dot{x}(t) \\ \dot{x}^{\mathrm{p}}(t) \end{bmatrix} = \begin{bmatrix} A & B^{\mathrm{p}} \\ 0 & A^{\mathrm{p}} \end{bmatrix} \begin{bmatrix} x(t) \\ x^{\mathrm{p}}(t) \end{bmatrix} + \begin{bmatrix} B^{\mathrm{c}} \\ 0 \end{bmatrix} u^{\mathrm{c}}(t) + \begin{bmatrix} w(t) \\ 0 \end{bmatrix}, \tag{15}$$

$$y(t) = \begin{bmatrix} C & D^{\mathrm{p}} \end{bmatrix} \begin{bmatrix} x(t) \\ x^{\mathrm{p}}(t) \end{bmatrix} + D^{\mathrm{c}}u^{\mathrm{c}}(t) + v(t). \tag{16}$$

The matrices B^{p} and D^{p} are given by:

$$B^{\mathrm{p}} = B^{\mathrm{c}}V \otimes \begin{bmatrix} 1 & 0 \end{bmatrix}, \quad D^{\mathrm{p}} = D^{\mathrm{c}}V \otimes \begin{bmatrix} 1 & 0 \end{bmatrix}, \tag{17}$$

with $\otimes$ being the Kronecker product and

$$V = \begin{bmatrix} V_1 & V_2 & \ldots & V_h \end{bmatrix}, \tag{18}$$

where $V_i \in \mathbb{R}^r$ for $i = 1,..,h$ are selection vectors with zeros and a one at the row relating to the control input on which the periodic disturbance acts. Note that, firstly, only the sine components of the periodic state act on the system and, secondly, as the disturbance is modelled on the control input, B^{c} and D^{c} are used instead of the generally unavailable B^{u} and D^{u}.

By discretization of (15)-(16), the following equations are now obtained:

$$\begin{bmatrix} x_{k+1} \\ x_{k+1}^{\mathrm{p}} \end{bmatrix} = \underbrace{\begin{bmatrix} A_{\mathrm{d}} & B_{\mathrm{d}}^{\mathrm{p}} \\ 0 & A_{\mathrm{d}}^{\mathrm{p}} \end{bmatrix}}_{\mathbf{A}} \underbrace{\begin{bmatrix} x_k \\ x_k^{\mathrm{p}} \end{bmatrix}}_{\mathbf{x}_k} + \underbrace{\begin{bmatrix} B_{\mathrm{d}}^{\mathrm{c}} \\ 0 \end{bmatrix}}_{\mathbf{B}} u_k^{\mathrm{c}} + \begin{bmatrix} w_k \\ 0 \end{bmatrix}, \tag{19}$$

$$y_k = \underbrace{\begin{bmatrix} C_{\mathrm{d}} & D_{\mathrm{d}}^{\mathrm{p}} \end{bmatrix}}_{\mathbf{C}} \begin{bmatrix} x_k \\ x_k^{\mathrm{p}} \end{bmatrix} + \underbrace{D_{\mathrm{d}}^{\mathrm{c}}}_{\mathbf{D}} u_k^{\mathrm{c}} + v_k, \tag{20}$$

where $\{\mathbf{A},\mathbf{B},\mathbf{C},\mathbf{D}\}$ denote the discrete state-space matrices of the augmented system with $\mathbf{x}_k$ being the augmented state, and w_k and v_k are assumed zero-mean Gaussian white noise sequences with finite fourth-order moments.

3.2 Kalman filter estimation of the input disturbance

An unbiased and minimum variance estimate of the states of the augmented state-space model (19)-(20) can be obtained using a Kalman filter (see e.g. Verhaegen and Verdult (2007)). The resulting state-space system has the following representation:

$$\hat{\mathbf{x}}_{k+1} = \mathbf{A}\hat{\mathbf{x}}_k + \mathbf{B}u_k^{\mathrm{c}} + K_k e_k, \tag{21}$$

$$y_k = \mathbf{C}\hat{\mathbf{x}}_k + \mathbf{D}u_k^{\mathrm{c}} + e_k, \tag{22}$$

where $\hat{(\bullet)}$ denotes an estimate, $K_k \in \mathbb{R}^{2n\times l}$ is the Kalman gain, and $e_k \in \mathbb{R}^l$ is the innovation signal. In order to calculate the Kalman gain, it is assumed that estimates of the covariance matrices of w_k and v_k are available:

$$\begin{bmatrix} R & S^T \\ S & Q \end{bmatrix} = E\left[\begin{bmatrix} v_k \\ w_k \end{bmatrix}\begin{bmatrix} v_j^T & w_j^T \end{bmatrix}\right] \geq 0, \quad \text{for } j = k. \tag{23}$$

The Kalman gain is then obtained through the Riccati difference equation:

$$P_{k+1} = \mathbf{A}P_k\mathbf{A}^T + Q - K_k(S + \mathbf{A}P_k\mathbf{C}^T)^T, \tag{24}$$

where P_k is the covariance matrix estimate. Proceeding, the gain is calculated as:

$$K_k = (S + \mathbf{A}P_k\mathbf{C}^T)(R + \mathbf{C}P_k\mathbf{C}^T)^{-1}. \tag{25}$$

The estimate of the periodic state $\hat{x}_k^{\mathrm{p}}$ can simply be extracted from $\hat{\mathbf{x}}_k$.

3.3 Phase Synchronization Wake Mixing Controller

This section presents a phase synchronization wake mixing controller that can be used to employ periodic wake mixing on downstream turbines in phase with the incoming wake. This is achieved by synchronizing the periodic control command with the periodic estimated input disturbance.

Using the Kalman filter, estimates of the periodic state $\hat{x}_k^{\mathrm{p}}$ can be found. Subsequently, the phase $\phi_{i,k}$ of each

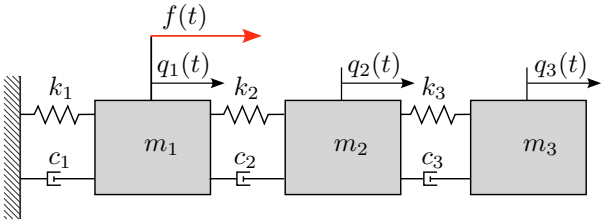

Fig. 3. Schematic of the simulated 3DOF system.

periodic signal $i = 1, .., h$ can be estimated by evaluating the following expression:

$$\phi_{i,k} = \text{atan2}\left(\frac{\hat{x}^{\text{p}}_{2i-1,k}}{\hat{x}^{\text{p}}_{2i,k}}\right). \tag{26}$$

Phase synchronization is then enabled by feeding the following command to the downstream controller:

$$u^{c}_{i,k} = a_i \sin \phi_{i,k}, \tag{27}$$

with a the desired amplitude. Note that any desired control action can be applied without affecting the phase estimate.

4. EVALUATION ON THREE-DEGREE-OF-FREEDOM SYSTEM

This section applies the proposed controller scheme (Fig. 2) to a three-degree-of-freedom mass-spring-damper system illustrated in Fig. 3. The system is composed of masses m_j, springs k_j, and dampers c_j, for $j = 1, 2, 3$. The masses are interconnected with one spring and damper; the first mass is connected to a fixed frame and the third is free. A periodic disturbance $f(t)$ excites the first mass. The mass, damping and stiffness matrices are given below:

$$M = \begin{bmatrix} m_1 & 0 & 0 \\ 0 & m_2 & 0 \\ 0 & 0 & m_3 \end{bmatrix}, \; J = \begin{bmatrix} c_1 + c_2 & -c_2 & 0 \\ -c_2 & c_2 + c_3 & -c_3 \\ 0 & -c_2 & c_3 \end{bmatrix},$$
$$K = \begin{bmatrix} k_1 + k_2 & -k_2 & 0 \\ -k_2 & k_2 + k_3 & -k_3 \\ 0 & -k_2 & k_3 \end{bmatrix}, \tag{28}$$

where $m_1 = 14$ kg, $m_2 = 16$ kg, $m_3 = 15$ kg, $c_1 = c_2 = c_3 = 0.6$ Ns/m, $k_1 = k_2 = 0.1$ N/m, and $k_3 = 0.3$ N/m. A Gaussian zero-mean white noise load disturbance w_k and output disturbance v_k with finite fourth-order moments are applied with covariance matrices $Q = R = 6\text{e}{-6}$ deg^2. A simulation is conducted for 2000 s with a sampling frequency of 125 Hz where the proposed control scheme estimates the periodic disturbance $f(t)$ and synchronizes the control action with this estimate.

Satisfactory results were obtained by tuning the Q and R matrices to $6\text{e}{-4}$ deg^2, where a root-mean-square error (RMSE) between the estimated and the actual signal of $9.89\text{e}{-2}$ deg was achieved with an initial phase offset of $\varphi = \pi/4$ (Table 1). An RMSE of $3\text{e}{-1}$ deg was achieved when a small phase perturbation of $\pi/6$ rad was applied at $t = 400$ s to test the estimator responsiveness.

Figure 4 displays the system response after the controller is activated at $t = 800$ s. For illustrative purposes, the controller was activated at the 800-second mark. Here, it can be observed that the output magnitude is amplified, indicating successful synchronization with the periodic

Table 1. Overview of parameters and RMSE.

Test	Q (deg^2)	R (deg^2)	RMSE (deg)
Normal	6e−4	6e−4	9.89e−2
Perturbed	6e−4	6e−4	3e−1

RMSE: root-mean-square error.

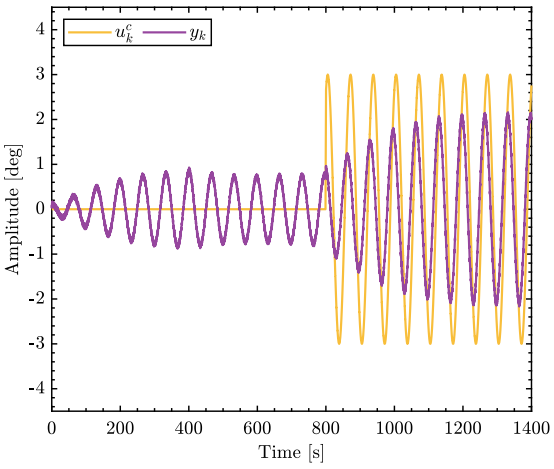

Fig. 4. The output signal y_k after the synchronized control command is applied from $t = 800$ s onwards.

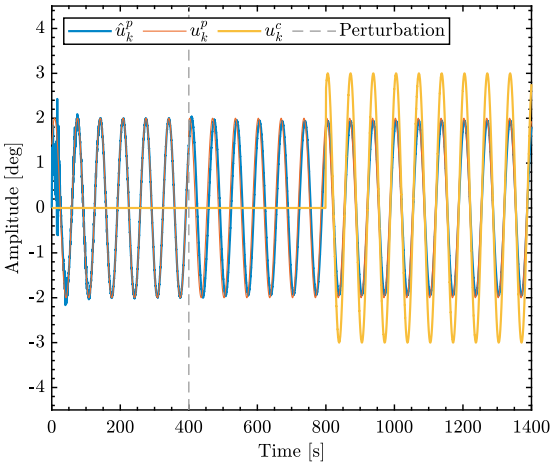

Fig. 5. Comparison of the estimated periodic input disturbance $\hat{u}^{\text{p}}_k$ against the actual disturbance u^{p}_k and the synchronized control input command u^{c}_k.

input disturbance. In Fig. 5, other relevant signals of this experiment are displayed. The figure qualitatively compares the estimate of the periodic input disturbance with the actual signal over the total simulation time. Also, the control signal is displayed, which can be observed correctly in phase with the periodic disturbance. Note that it takes several cycles for the phase perturbation at $t = 400$ s to be corrected. As a comparison, the system response when the control command is not synchronized and out of phase is displayed in Fig. 6, clearly indicating the necessity of phase synchronization.

5. CONCLUSIONS

Current research does not yet apply wake mixing control on downstream turbines, while it is expected that significant benefits can be gained from this. The periodic

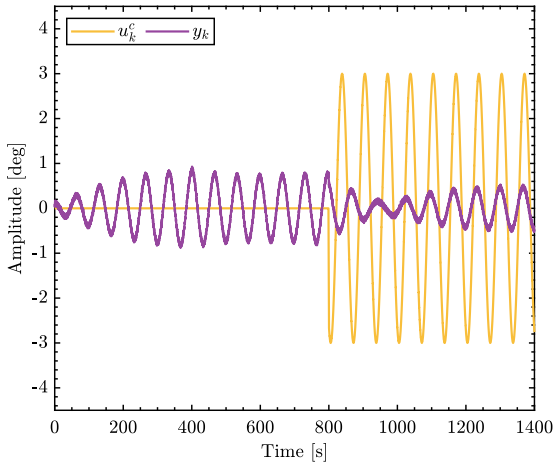

Fig. 6. The output signal y_k after the control command is applied out of phase from $t = 800$ s onwards.

component present in the helix wake experienced by the downstream turbine may be leveraged to reduce its control actions for wake mixing. This work studied this case by abstracting the downstream turbine to a mass-spring-damper system and modelling the periodic component of the wake as an input disturbance on the control input.

A novel disturbance estimator with a phase synchronization control scheme was derived to estimate the periodic input disturbance. An evaluation on a three-degree-of-freedom mass-spring-damper system was performed as proof of principle, demonstrating low estimation error even with a small phase perturbation. Future work should demonstrate the full potential of the proposed control scheme in wind turbine simulations and experimental studies preserving actual operating conditions.

ACKNOWLEDGMENT

This work is part of the Hollandse Kust Noord wind farm innovation program where CrossWind C.V., Shell, Eneco and Siemens Gamesa are teaming up; funding for the PhDs was provided by CrossWind C.V. and Siemens Gamesa.

REFERENCES

Annoni, J., Gebraad, P.M., Scholbrock, A.K., Fleming, P.A., and Wingerden, J.W.v. (2016). Analysis of axial-induction-based wind plant control using an engineering and a high-order wind plant model. *Wind Energy*, 19(6), 1135–1150.

Barthelmie, R.J., Hansen, K., Frandsen, S.T., Rathmann, O., Schepers, J., Schlez, W., Phillips, J., Rados, K., Zervos, A., Politis, E., et al. (2009). Modelling and measuring flow and wind turbine wakes in large wind farms offshore. *Wind Energy*, 12(5), 431–444.

Fleming, P.A., Gebraad, P.M., Lee, S., van Wingerden, J.W., Johnson, K., Churchfield, M., Michalakes, J., Spalart, P., and Moriarty, P. (2014). Evaluating techniques for redirecting turbine wakes using sowfa. *Renewable Energy*, 70, 211–218.

Frederik, J.A., Doekemeijer, B.M., Mulders, S.P., and van Wingerden, J.W. (2020). The helix approach: Using dynamic individual pitch control to enhance wake mixing in wind farms. *Wind Energy*, 23(8), 1739–1751.

Frederik, J.A. and van Wingerden, J.W. (2022). On the load impact of dynamic wind farm wake mixing strategies. *Renewable Energy*.

Global Wind Energy Council (2022). Global wind report 2022. Technical report, GWEC.

Goit, J.P. and Meyers, J. (2015). Optimal control of energy extraction in wind-farm boundary layers. *Journal of Fluid Mechanics*, 768, 5–50.

González-Longatt, F., Wall, P., and Terzija, V. (2012). Wake effect in wind farm performance: Steady-state and dynamic behavior. *Renewable Energy*, 39(1), 329–338.

Greś, S., Döhler, M., Andersen, P., and Mevel, L. (2021). Kalman filter-based subspace identification for operational modal analysis under unmeasured periodic excitation. *Mechanical Systems and Signal Processing*, 146, 106996.

Meyers, J., Bottasso, C., Dykes, K., Fleming, P., Gebraad, P., Giebel, G., Göçmen, T., and van Wingerden, J.W. (2022). Wind farm flow control: prospects and challenges. *Wind Energy Science*, 7(6), 2271–2306.

Ni, B. and Zhang, Q. (2013). Kalman filter for process noise free systems. *IFAC Proceedings Volumes*, 46(11), 176–181.

Pamososuryo, A.K., Mulders, S.P., Ferrari, R., and van Wingerden, J.W. (2022). Periodic load estimation of a wind turbine tower using a model demodulation transformation. In *2022 American Control Conference (ACC)*, 5271–5276.

Pörtner, H.O., Roberts, D.C., Adams, H., Adler, C., Aldunce, P., Ali, E., Begum, R.A., Betts, R., Kerr, R.B., Biesbroek, R., et al. (2022). Climate change 2022: Impacts, adaptation and vulnerability. *IPCC Sixth Assessment Report*.

Simley, E. and Pao, L.Y. (2016). Evaluation of a wind speed estimator for effective hub-height and shear components. *Wind Energy*, 19(1), 167–184.

Siemens Gamesa (2019). URL `https://www.siemensgamesa.com/en-int/newsroom/2019/11/191126-siemens-gamesa-wake-adapt-en`.

van der Hoek, D., Kanev, S., Allin, J., Bieniek, D., and Mittelmeier, N. (2019). Effects of axial induction control on wind farm energy production-a field test. *Renewable energy*, 140, 994–1003.

Van Kuik, G., Peinke, J., Nijssen, R., Lekou, D., Mann, J., Sørensen, J.N., Ferreira, C., van Wingerden, J.W., Schlipf, D., Gebraad, P., et al. (2016). Long-term research challenges in wind energy–a research agenda by the european academy of wind energy. *Wind energy science*, 1(1), 1–39.

van Vondelen, A.A.W., Navalkar, S.T., Kerssemakers, D.R.H., and van Wingerden, J.W. (2023). Enhanced wake mixing in wind farms using the helix approach: A loads sensitivity study. In *2023 American Control Conference (ACC)*. AACC, San Diego, California, USA.

Verhaegen, M. and Verdult, V. (2007). *Filtering and system identification: a least squares approach*. Cambridge university press.

Zheng, L., Geng, H., and Yang, G. (2016). Fast and robust phase estimation algorithm for heavily distorted grid conditions. *IEEE Transactions on industrial electronics*, 63(11), 6845–6855.